



**HAL**  
open science

## Snow particle speeds in the blowing snow

K. Nishimura, C. Yokoyama, Y. Ito, M. Nemoto, F. Naaim-Bouvet, H. Bellot,  
K. Fujita

► **To cite this version:**

K. Nishimura, C. Yokoyama, Y. Ito, M. Nemoto, F. Naaim-Bouvet, et al.. Snow particle speeds in the blowing snow. International Snow Science Workshop (ISSW), Oct 2013, Grenoble – Chamonix Mont-Blanc, France. p. 147 - p. 153. hal-00950057

**HAL Id: hal-00950057**

**<https://hal.science/hal-00950057>**

Submitted on 20 Feb 2014

**HAL** is a multi-disciplinary open access archive for the deposit and dissemination of scientific research documents, whether they are published or not. The documents may come from teaching and research institutions in France or abroad, or from public or private research centers.

L'archive ouverte pluridisciplinaire **HAL**, est destinée au dépôt et à la diffusion de documents scientifiques de niveau recherche, publiés ou non, émanant des établissements d'enseignement et de recherche français ou étrangers, des laboratoires publics ou privés.

## Snow particle speeds in the blowing snow

Kouichi Nishimura<sup>1</sup>, Chika Yokoyama<sup>1</sup>, Yoichi Ito<sup>1</sup>, Masaki Nemoto<sup>2</sup>,  
Florence Naaim-Bouvet<sup>3</sup>, Hervé Bellot<sup>3</sup>, Koji Fujita<sup>1</sup>  
<sup>1</sup>Nagoya University, Nagoya, Japan  
<sup>2</sup>Snow and Ice Research Center, NIED, Japan  
<sup>3</sup>UR ETNA, IRSTEA, Saint-Martin d'Hères, France

**ABSTRACT:** Snow particle speeds are one of the key issues in order to deepen our understanding for the internal structures of blowing snow. In this study, we utilized the snow particle counter (SPC) developed to observe the snow particle size distribution and the mass flux every one second. We have recorded the direct output signal from the transducer with high frequency, and obtained the particle size and the duration of time when the individual particle passed the sampling area. Then, utilizing two data the particle speeds are calculated.

Firstly, measurements were carried out at Lac Blanc Pass in French Alps. Then, more precise measurements were conducted at the cold wind tunnel in NIED, which is 14 m long and its working section is 1 m x 1 m. Snow particle speed, its distribution with height and the relation to the wind speeds showed good agreement; the snow particle speed and the wind speed increased with height, and the former was always smaller than the latter below 1 m. In this manner, we succeeded to obtain the reliable snow particle speeds in the blowing snow for the first time and revealed its grain size dependence and the relation to the wind speeds.

Similar trends were also shown with the random flight calculations; particle speeds are lower than the air speed. However, the differences in wind and particle speeds amounted larger in the simulation.

**KEYWORDS:** blowing snow, snow particle speed, wind speed, snow particle counter (SPC)

### 1 INTRODUCTION

The blowing snow is a leading agent for dynamics of numerous climatic and hazardous processes and a number of researches have been carried out so far. However, our understandings for the internal structures of blowing snow are still far from satisfactory.

Numerical blowing snow model can be a useful tool to investigate the blowing snow phenomena as well as the field observations and the wind tunnel experiments. However, numerous improvements are still necessary at this stage. For instance, in the turbulent diffusion model (such as Uematsu, 1993; Naaim et al., 1998, Gauer, 1998; Dery and Yau, 1999; Bintanja, 2001), the air and snow particles are usually assumed to behave in the same manner; in some cases specific constant are set for the Schmidt number which is the ratio between the diffusion coefficient of air and snow particles (Dery et al., 1998), or particle fall speeds are assumed to fit the observed concentrations. On the other hand, in the random flight model (Nemoto and Nishimura, 2004), which takes into account the turbulence and the particle inertia,

and describes the individual particle motion, several assumptions and unknown arbitrary parameters are still involved in. Particle speeds in the blowing snow are one of the key issues in the both models.

Nishimura and Hunt (2000) obtained the speeds of saltating snow particle in the wind tunnel. Trajectories of the particles were recorded with the stroboscopic light and high speed video system, and analyzed to deduce the particle speeds for ascending and descending particles. However, particle concentration becomes larger with increasing the friction velocity  $u_*$ , and it became difficult to distinguish individual particles;  $u_*$  was limited around the threshold. In addition, we could not detect smaller particles in this technique. Thus, particle size dependencies were hard to discuss.

Recently the leading edge technologies, such as laser doppler anemometry (LDA), particle image velocimetry (PIV) and particle-tracking velocimetry (PIV), have applied to measure the sand particle speeds in the saltation layer (Liu and Dng, 2004; Rasmussen and Sorensen, 2005; Yang et al., 2007; Creyssels et al., 2009). However, size dependencies on particle speed were still hard to reveal. Further, all the measurements were limited in the wind tunnel scale and no measurements in the field were conducted. In this study, we utilized the snow particle counter (SPC) developed to observe the snow particle size distribution and the mass flux

---

*Corresponding author address:*

Kouichi Nishimura, Nagoya University,  
Furo-cho, Chikusa-ku Nagoya, 464-8601, JAPAN  
tel: +81 52 789 3480; fax: +81 52 789 3480  
email: knishi@nagoya-u.jp

every one second (Sato et al., 1993). We have recorded the raw output signal from the transducer with high frequency, and obtained the particle size and the duration of time when the individual particle passed the sampling area. Then, the particle speeds were calculated.

Firstly measurements were carried out with three SPCs at Col du Lac bran in French Alps in March, 2012. Then, more precise measurements were conducted at the cold wind tunnel in NIED, which is 14 m long and its working section is 1 m x 1 m. Obtained results were compared with the random flight calculations (Nemoto and Nishimura, 2004) as well.

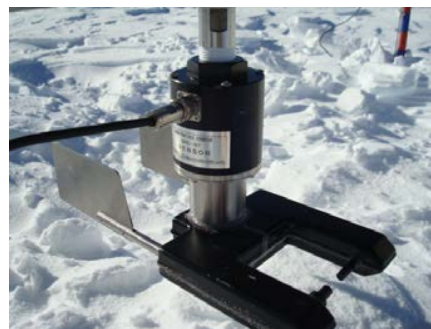


Figure 1. Snow particle counter (SPC)

## 2 INSTRUMENTS AND METHODS

### 2.1 Snow particle counter (SPC)

The snow particle counter (SPC, Niigata Denki Co.) (Figure 1) is an optical device (Nishimura and Nemoto, 2005). The diameter and the number of blowing snow particles are detected by their shadows on photodiode. Electric pulse signals of snow particles passing through a sampling volume ( $2 \times 25 \times 0.5$  mm) are sent to a transducer and an analyzing data logging system (PC). In this way the snow particle counter detects particles between 40 and 500  $\mu\text{m}$  in mean diameter. It divides them into 32 classes and records the particle number every one second. The SPC has a self-steering wind vane. The sampling area, perpendicular to horizontal wind vector is 50 mm<sup>2</sup> ( $2 \times 25$  mm). If the diameter of a snow particle is larger than the maximum diameter class, the snow particle is considered to belong to the maximum diameter class. In usual, SPC is applied to observe the snow particle size distribution and mass flux. However, when we get the direct output signal from the transducer with high frequency (ex. 150 kHz for the field measurement and 100 kHz for the wind tunnel experiment in this study), the wave form is given as Figure 2. The peak corresponds to the particle size  $d$  and  $t$  is the duration of time in which the particle passed the sampling area. Then the particle speeds can be calculated with equation 1 in principle.

$$v = \frac{L+d}{t} \quad (1)$$

Here  $L$  ( $=500 \mu\text{m}$ ) is the width of the sampling area.

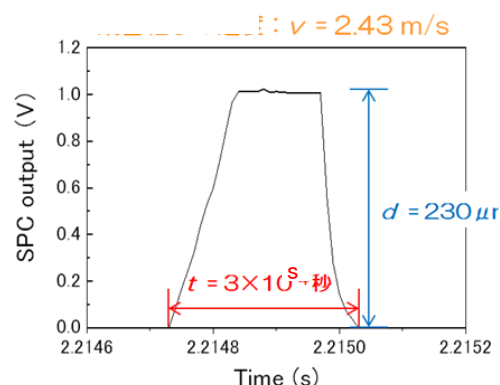


Figure 2. Wave form from SPC

### 2.2 Field measurements

Firstly measurements were carried out at Lac Blanc Pass in French Alps. It is a large north-south-oriented pass located at 2720 m a.s.l., near Alpe d'Huez ski resort. It consists of relatively flat terrain over a length of about 300 m where blowing snow has been studied for twenty years by IRSTEA (formerly Cemagref) and Météo France. Due to surrounding topography, 90% of observed winds blow from North-East or South. Three SPCs were installed on a mast as shown in Figure 3. One was set up at a fixed position (3.42 m above the snow surface). Two others were near the snow pack surface and could be adjusted manually; a fixed distance of 1.02 m separates them. Outputs from the SPCs were recorded for 100s at 150 kHz. Two cup anemometers (AF860, Makino Applied Instruments Inc.) were set at 1.37 m and 0.35 m respectively. Further, an ultrasonic anemometer (USA-1, Metek) gave the wind speeds of 2.17 m high. Measurements were carried out on 5 March, 2012.



Figure 3. Experimental set up at Lac Blanc Pass

### 2.3 Wind tunnel experiments

Experiments were conducted in a cold wind-tunnel at the Cryospheric Environmental Simulator (CES) in Shinjo, Japan (Figure 4). The test section of the wind-tunnel was 14 m long, 1 m wide, and 1 m high. The temperature was kept at constant  $-15^{\circ}\text{C}$ . In order to initiate and maintain steady saltation, seed particles were supplied from the bottom of the wind tunnel entrance at a constant rate. Further details of the wind tunnel are described in Sato et al. (2001). As shown in Figure 4, the SPC and an ultrasonic anemometer (TR-92T, Kaijo Co.) were set 0.2 m apart at a same height from the snow surface. Measurements were taken under varying conditions of wind speed of 8, 10 and  $12\text{ m s}^{-1}$  at the centre of wind tunnel and height of sensors from 0.015 to 0.15 m from the surface. Although most of the measurements were conducted at 12 m leeward from the wind tunnel entrance and additional experiments were also done at 6 m.



Figure 4. Cold wind-tunnel at CES

## 3 RESULTS

### 3.1 Field measurements

Although measurements were conducted for eight times, here we introduce six cases when the snow precipitation was not observed. As is stated, all the data were recorded for 100 s, however the wind speed changed largely during

the measurement. Thus, in the analysis, two to ten seconds data, during which the wind speed was almost constant, were extracted. Hereafter, we call them as case A to F respectively. Figure 5 shows examples of snow particle diameter distributions and the horizontal mass flux measured using the SPCs. At case A, when the wind speed at 2.17 m high was around  $10\text{ m/s}$ , the particle diameter is widely distributed within a range of 50 to  $500\text{ }\mu\text{m}$ . However, with increasing height, the proportion of small particles, particularly less than  $100\text{ }\mu\text{m}$  in diameter, becomes dominant. The horizontal mass flux showed the exponential decay with height, as a number of researchers have previously found (Takeuchi 1980, Nishimura and Nemoto 2005).

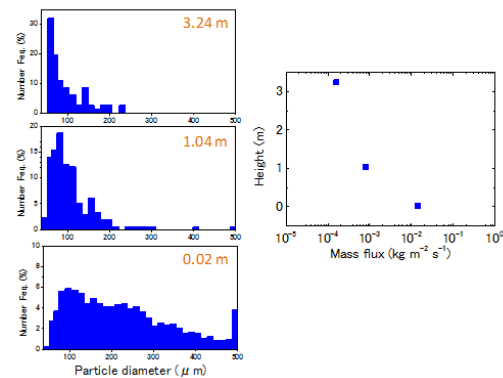


Figure 5. Snow particle diameter distributions and the horizontal mass flux at case A

Snow particle speeds obtained with high frequency sampling of SPCs data were shown as a function of height in Figure 6. Wind speeds measured with the ultrasonic anemometer and the cup anemometers are also plotted. In all cases, the wind speeds and the particle speeds increased monotonously with height although the fluctuations of latter are fairly large. Generally the wind speed was higher than the wind speed at each measuring point. It should be also noted that the difference seems getting smaller with decreasing height, which suggests both agrees each other at close to the snow surface; in fact, the particle speed became slightly larger than the wind speed at 0.3 m in case D.

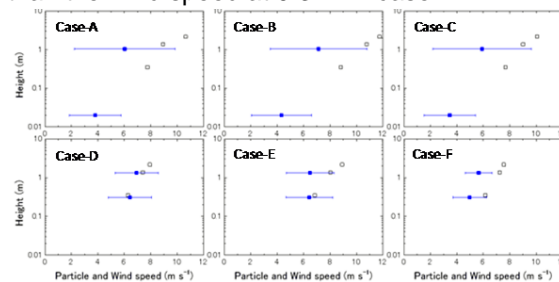


Figure 6. Snow particle speed (■: average and standard deviation) and wind speed (□: average) distribution in the blowing snow.

### 3.2 Wind tunnel experiments

Figure 7 indicates the snow particles and their diameter distributions for 2929 samples used in the wind tunnel experiments. The latter can be accurately approximated by means of the two-parameter gamma probability density function (Budd 1966, Schmidt 1982),

$$f(D) = \frac{d^{\alpha-1}}{\beta^\alpha \Gamma(\alpha)} \exp\left(-\frac{\beta}{D}\right) \quad (2)$$

Where  $d$  is the particle diameter,  $\alpha$  is the shape parameter which determines the skewness of the distribution and  $\beta$  is the shape parameter which describes the width/scale of the distribution. Since the mean and variance are  $\alpha\beta$  and  $\alpha\beta^2$ , respectively, both parameters can be easily evaluated. In this study  $\alpha$  was obtained as 3.25 and  $\beta$  was 127.80.

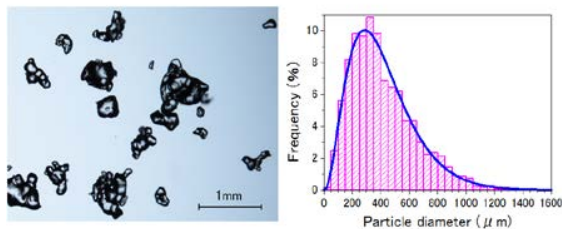


Figure 7. Snow particles and diameter distributions used in the wind tunnel experiments.

Figure 8 shows the particle size and the horizontal mass flux distributions as a function of height when the wind speed at the centre of wind tunnel was  $8 \text{ m s}^{-1}$ . The drifting snow particles indicated broad distribution near the snow surface (0.015 m). Frequencies of smaller particles become dominant with increasing height as was also shown in the field measurement (Figure 5). Horizontal mass flux showed the exponential decay with height, as was also shown in Figure 5. Same trends are observed for all experiments with different wind speeds and locations.

On the other hand, Figure 9 introduces the particle speeds and the wind speeds distributions measured with the SPC and the ultrasonic anemometer respectively, when the wind speed at centre of wind tunnel was 8, 10 and  $12 \text{ m s}^{-1}$ , which correspond to the friction velocity  $u_*$  of 0.37, 0.45 and  $0.63 \text{ m s}^{-1}$  respectively. At  $u_*$  was  $0.37 \text{ m s}^{-1}$ , wind speeds became larger from 4.8 to  $6.2 \text{ m s}^{-1}$  with height of 0.03 m to 0.15 m, and the particle speeds also showed monotonous increase with height (ex.  $3.2 \text{ m s}^{-1}$  at 0.0015 m and  $5 \text{ m s}^{-1}$  at 0.1 m) although the scattering of latter was fairly large (nearly  $2 \text{ m s}^{-1}$ ). Point is that the particle speeds were less than the wind speeds within the measured height. Above

trends are recognized for other two cases of wind speeds, in spite the difference between the wind speeds and the particle speeds became larger at larger wind speeds.

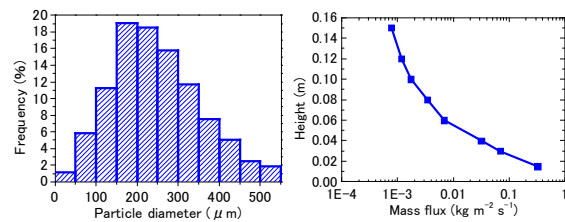


Figure 8. Particle size at 0.015 m high and horizontal mass flux distributions at  $u_* = 0.37 \text{ m s}^{-1}$ .

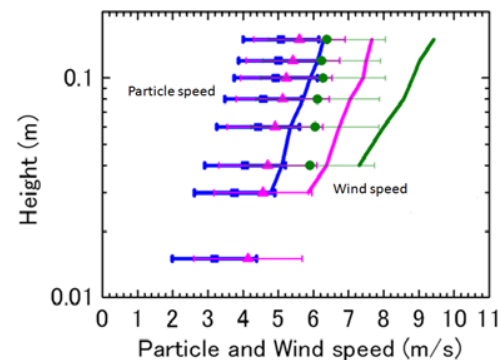


Figure 9. Particle and wind speed distributions at  $u_* = 0.37$  (blue), 0.45 (red) and  $0.63 \text{ m s}^{-1}$  (green).

Figure 10 indicates an example how the particle speeds changed with the particle diameter, at 0.015 m high and  $u_* = 0.37 \text{ m s}^{-1}$ . Mean particle speeds decreased clearly from  $6 \text{ m s}^{-1}$  to  $2 \text{ m s}^{-1}$  as the particle diameter became larger. If we assume the wind speed profile keeps the similar trend in Figure 9 and can be extrapolated to lower height, the wind speed at 0.015 m high will be around  $4 \text{ m s}^{-1}$ . Thus, Figure 10 suggests that the smaller particles less than  $100 \mu\text{m}$  diameter moved faster than the wind speed, whereas the larger ones vice versa at 0.015m high.

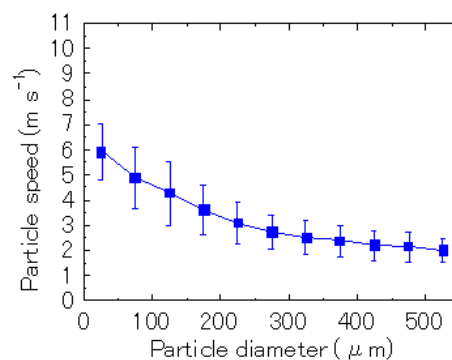


Figure 10. Snow particles speeds at 0.015 m high as a function of diameter. ( $u_* = 0.37 \text{ m s}^{-1}$ )



## 4 DISCUSSIONS

### 4.1 Comparisons between the field measurements and the wind tunnel experiments

In this paragraph, we compare the measurements at Lac Blanc Pass and the wind tunnel experiments at CES.

Figure 11 shows the particle diameter distributions measured individually: 0.02 m high in the field (case B) in which the wind speed at 2.17 m high was around  $10 \text{ m s}^{-1}$ , whereas 0.015 m high in the wind tunnel and  $u_*$  was  $0.37 \text{ m s}^{-1}$ . The maximum frequency can be found around  $100 \mu\text{m}$  in the field, while  $150$  to  $250 \mu\text{m}$  in the wind tunnel. Further, the former looks more skewed than the latter. Probably these caused the differences in the horizontal mass flux as shown in Figure 12. Near the snow surface, fluxes in the wind tunnel was about one order of magnitude larger than the field and decreased more rapidly with height. However, the wind speed profile for both cases can be recognized reasonably the same in Figure 13 and we see the particle speeds are almost within the equivalent range. Although the scale of the field measurements and the wind tunnel experiments were different, the particle speeds distributions obtained with both approaches agreed fairly well under the same wind profile, that is, the same friction velocity. It suggests that the procedures introduced in this study are consistent and we wish to stress that we successfully revealed the particle speed in the blowing snow and its dependencies on the height from the snow surface, particle size, and the wind speeds.

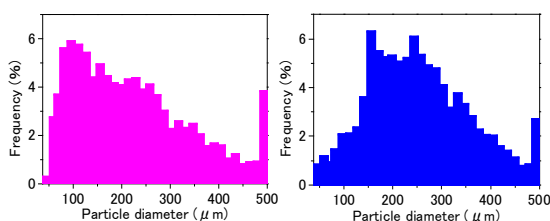


Figure 11. Particle diameter distributions. Left: at 0.02 m high in the field (case B), the wind speed at 2.17 m high was around  $10 \text{ m s}^{-1}$ , Right: at 0.015 m high in the wind tunnel and  $u_*$  was  $0.37 \text{ m s}^{-1}$ .

Further, we can conclude that under this condition, particle speeds are always from  $1$  to  $2 \text{ m s}^{-1}$  lower than the wind speeds within the region of  $0.015$  to  $1 \text{ m}$  high, that is, the momentum are transferred from the wind to particles here.

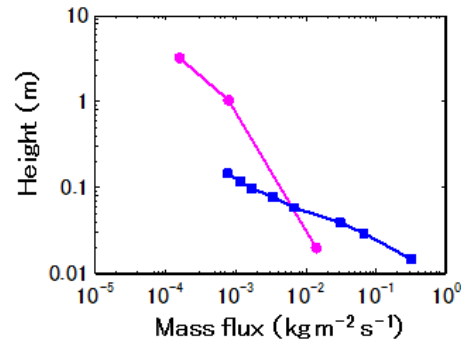


Figure 12. Horizontal snow mass flux profiles. Red: field measurement (case B), Blue: wind tunnel experiments. Wind speeds are the same as Figure 11.

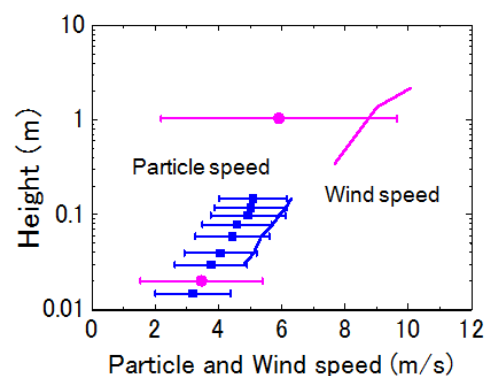


Figure 13. Particle and wind speed distributions. Red: field measurement (case B), Blue: wind tunnel experiments. Wind speeds are the same as Figures 11 and 12.

### 4.2 Comparisons between the wind tunnel experiments and the numerical simulations

Nemoto and Nishimura (2004) have developed a numerical drifting snow model which incorporates the turbulence action based on the Random Flight model in order to discuss both the saltation and the suspension modes together. All of the physical processes including aerodynamic entrainment, the grain/bed collision, wind modification, particle size distribution, and the turbulent fluctuations on the particle trajectories are taken into consideration. Detailed explanation of the blowing snow model and the simulation procedure used in this study have been provided in Nemoto (2002) and Nemoto and Nishimura (2004).

In this study we substitute the parameters into the model, based on the wind tunnel experiments, that is the friction velocity of  $0.37 \text{ m s}^{-1}$ , roughness length of  $1.82 \times 10^{-5} \text{ m}$  and the particle size distribution parameters of  $\alpha$  and  $\beta$  obtained in Figure 7, and used the computational

results when the flux distribution arrived at a steady state.

Computed horizontal mass flux profiles are shown in Figure 14 and are compared with the profiles observed with the wind tunnel experiment at  $u_* = 0.3 \text{ m s}^{-1}$ . The computations and the experiments closely agree not only qualitatively but also quantitatively, although a slight departure above 0.1 m high is seen. In Figure 15, particle speeds and wind speeds calculated are plotted. In the calculation, at higher than 0.1 m, the wind speeds and the particle ones are almost the same which implies that the air and the drifting and blowing snow particles behave in the same manner. On the other hand, below 0.1 m, particle speeds become lower than the air speed. So the momentum is transferred from the wind to particles here. On the contrary, although it is not shown in Figure 15, very close to the surface at less than 1 mm, particle speeds are getting higher than the wind speed. It is probably because descent particles from higher position have larger momentum in general.

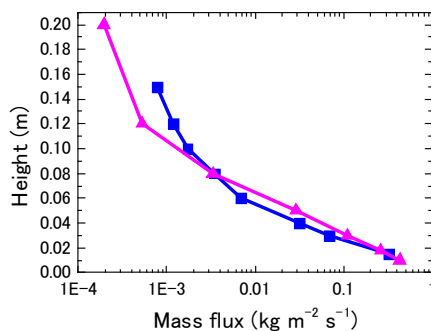


Figure 14. Horizontal mass flux profiles. Red: calculated one at  $u_*$  is  $0.37 \text{ m s}^{-1}$ , Blue: wind tunnel experiment at the same conditions.

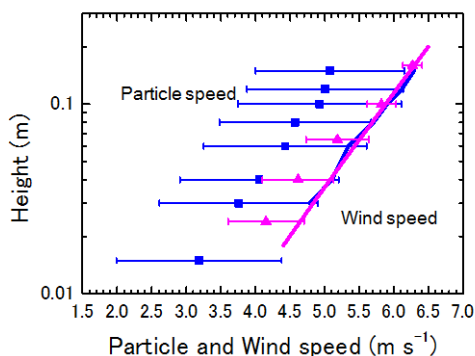


Figure 15. Particle and wind speed distributions. Red: calculated, Blue: wind tunnel experiments. Conditions are the same as Figure 14.

On the other hand, when we compare the computations by the random flight model with the wind tunnel ones carried out under the same

conditions, two approaches don't always agree. Wind speed profiles showed a good agreement. Further, both the snow particle speed and the wind speed increased with height, and the former is smaller than the latter below 0.1 m high in both cases. However, it should be noted that the calculated particle speeds are always larger than the measurements. Differences seem to increase with height. Figure 16 also indicates that the calculated speeds are higher than the measured ones for all particle sizes except for the smallest particles that is less than  $50 \mu\text{m}$ .

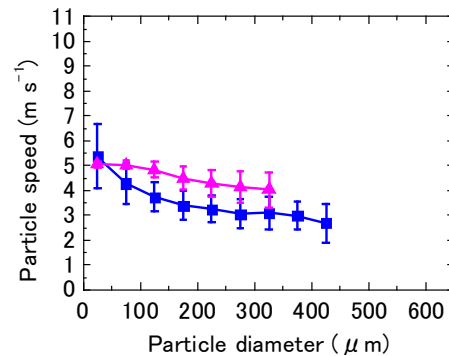


Figure 16. Snow particles speeds at 0.04 m high as a function of diameter. Red: calculated, Blue: wind tunnel experiments. Conditions are the same as Figures 14 and 15.

Above discrepancies between the experiments and computations suggest that the physical sub-processes involved in the model should be examined more carefully. The fact, that the particle speeds differed largely, even though the flux agreed fairly well, implies that the particle size distributions in the air are not calculated precisely. Thus, we need to reconsider the effect of turbulence, particle inertia, and particle pick up process from the snow surface more carefully.

In addition, we need to factor in the effects of wind tunnel length as well. As is described, supplementary experiments were also carried out at 6 m leeward from the wind tunnel entrance. Figure 17 shows the obtained compared with the ones at 12 m. We can recognize clearly that both wind and particle speeds at 12 m are larger than the ones at 6 m. It suggests the blowing snow is still in the developing stage at 6 m at least, although Kosugi *et al.* (2005) reported that the horizontal mass flux profile became nearly the same at more than 2 m from the entrance. If the blowing snow has not arrive at the steady state yet even at 12 m, the particle speeds may increase more or less at leeward and possibly become closer to the calculated ones. Particle shape is also needed to be taken into consideration. In the calculation, the snow

particles are assumed to be spheres and the drag force acting on the particles are obtained, however, it is not always the case as shown in Figure 7. Further, only the translational particle motion is involved in the calculation; no rotation was considered. If the momentum transferred from the wind are spent for both translation and rotation, and they are included in the model, the calculated translational particle speeds may decrease and the amount of differences found in Figures 15 and 16 can be smaller.

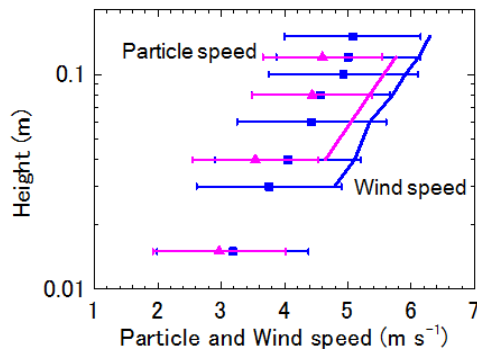


Figure 17. Particle and wind speed distributions at  $u_* = 0.37 \text{ m s}^{-1}$ .  
Red: 6 m leeward from the wind tunnel entrance, Blue: 12 m.

## 5 ACKNOWLEDGMENTS

The authors are grateful to all of their colleagues who participated in the field measurements and the wind-tunnel experiments. Certainly, the work could not have been completed without their cooperation.

## 6 REFERENCES

- Bintanja, R., 2001. Characteristics of snowdrift over a bare ice surface in Antarctica. *J. Geophys. Res.*, 106: 9653-9659.
- Budd, W. F., 1966. The drifting of non-uniform snow particles. In *Studies in Antarctic meteorology* (ed. Rubin, M. J.), Antarctic Research Series: Vol. 9, pp. 59-70. Washington, DC: American Geophysical Union.
- Creysseles, M., Dupont, P., Ould, El Moctar, A., Valance, A., Cantat, I., Jenkins, J. T., Pasini, J. M. and Rasmussen K. R., 2009. Saltating particles in a turbulent boundary layer: experiment and theory. *J. Fluid mech.* 625: 47-74.
- Dery, S. J., Taylor, P. A. and Xiao, J., 1998. The thermodynamic effects of sublimating, blowing snow in the atmospheric boundary layer. *Boundary-Layer Meteorol.*, 89: 251-283.
- Dery, S. J. and Yau, M. K., 1999. A bulk blowing snow model, *Boundary-Layer Meteorol.*, 93: 237-251.
- Gauer, P., 1998. Blowing and drifting snow in Alpine terrain: numerical simulation and related field measurements. *Ann. Glaciol.*, 26: 174-178.
- Kosugi, K., Sato, T., Masaki, N., Nishimura, K., Sato, A. and Mochizuki, S., 2005. Wind-tunnel experiments on the development of drifting snow (12) – Changes in mass flux vertical distribution at different particle diameters in drifting snow with horizontal distance. Preprints of the 2005 Conference Japanese Society of Snow and Ice, B4-13 (in Japanese).
- Liu, V. and Dong, Z., 2004. Vertical profiles of Aeolian sand mass flux. *Geomorphology*, 59: 205-219.
- Naaim, M., Naaim-Bouvet, F. and Martinez, H., 1998. Numerical simulation of drifting snow: erosion and deposition models. *Annals of Glaciology*, 26: 191-196.
- Nemoto, M., 2002. Dynamics of drifting snow particles in turbulent boundary-layer. Ph. D. thesis, Graduate School of Environmental Earth Science, Hokkaido University, Japan, 98 pp.
- Nemoto, M and Nishimura, K. 2004. Numerical simulation of drifting snow in turbulent boundary layer. *J. Geophys. Res.*, 109: D18206. (doi:10.1029/2004JD004657)
- Nishimura, K. and Hunt J. C. R., 2000. Saltation and incipient suspension above a flat particle bed below a turbulent boundary layer. *J. Fluid. Mech.*, 417: 77-102.
- Nishimura, K. and Nemoto M., 2005. Blowing snow at Mizuho station, Antarctica. *Philosophical Transactions of the Royal Society, A* 363: 1647-1662.
- Rasmussen, K. R. and Sorensen M., 2005. Dynamics of Particles in Aeolian saltation: Powder and Grains (Ed. Garcia-Rojo, R., Herrmann, H. J. and McNamara, S.) pp. 967-971. A. A. Balkema Publishers.
- Sato, T., Kimura, T., Ishimaru, T. and Maruyama, T., 1993. Field test of a new snow-particle counter (SPC) system. *Annals of Glaciology*, 18: 149-154.
- Sato, T., Kosugi, K., and Sato A., 2001. Saltation-layer structure of drifting snow observed in a wind tunnel. *Annals of Glaciology*, 32: 203-208.
- Schmidt, R. A., 1982. Vertical profiles of wind speed, snow concentration, and humidity during blowing snow. *Boundary layer Meteorol.*: 23, 223-246.
- Takeuchi, M., 1980. Vertical profile and horizontal increase of drift-snow transport. *J. Glaciol.*, 26 (94): 481-492.
- Uematsu, T., 1993. Numerical study on snow transport and drift formation. *Ann. Glaciol.*, 18: 135-141.
- Yang, P., Dong, Z., Qian, G., Luo, W. and Wang, H., 2007. Height profile of the mean velocity of an aeolian saltating cloud: wind tunnel measurements by particle image velocimetry. *Geomorphology* 89: 320-334.